JOURNAL OF MATERIALS SCIENCE **38** (2003) 3973–3978

Hydrothermal preparation of mesoporous TiO_2 powder from $Ti(SO_4)_2$ with poly(ethylene glycol) as template

RUIQIN TAN
Department of Chemistry, Tsinghua University, Beijing 100084, People's Republic of China; State Key Laboratory of C1 Chemical Engineering, Tsinghua University, Beijing 100084, People's Republic of China

YU HE
Department of Chemistry, Tsinghua University, Beijing 100084, People's Republic of China

YONGFA ZHU*
Department of Chemistry, Tsinghua University, Beijing 100084, People's Republic of China; State Key Laboratory of C1 Chemical Engineering, Tsinghua University, Beijing 100084, People's Republic of China
E-mail: zhuyf@chem.tsinghua.edu.cn

BOQING XU
State Key Laboratory of C1 Chemical Engineering, Tsinghua University, Beijing 100084, People's Republic of China

LILI CAO
Department of Chemistry, Tsinghua University, Beijing 100084, People's Republic of China

Mesoporous titania powder with anatase structure was prepared by hydrothermal synthesis from low-cost $Ti(SO_4)_2$ water solution with nontoxic poly ethylene glycol (PEG) as a templating agent. The templating pathway was suggested to use hydrogen bonding interaction between the hydrophilic surfaces of flexible rod- or worm-like micelles and the hydrothermal products of $Ti(OH)_4$ to assemble an inorganic oxide framework. The mesoporous channel structures with diameters about 3 nm to 18 nm were achieved by adding appropriate amount of PEG with average moelcular weight of 200. The obtained powder showed good performance for the degradation of gaseous formaldehyde. These results suggested that hydrothermal synthesis with PEG templating provided a low-cost and convenient pathway to synthesis mesoporous TiO_2 powder from water solution system. © *2003 Kluwer Academic Publishers*

1. Introduction

Titania has been accepted as one of the best photocatalysts for the degradation of environmental contaminants owing to its nontoxicity, long-term stability and convenient band-gap energy [1]. The photocatalytic activity of TiO_2 depends upon its crystal structure (anatase or rutile), specific surface area, pore size distribution, presence of dopants and surface hydroxyl group density [2–5]. Mesoporous titania shows fairly high activity in photocatalysis performance due to its high specific surface area. An easy and convenient preparation method to obtain titania with high porosity, high homogeneity and high surface area is desirable.

There are several ways of preparing TiO_2 particles and films, such as chemical vapor deposition using $TiCl_4$ as raw material, sol-gel method using titanium alkoxide as raw material or titanium alkoxide hydrolysis method [6–10]. Among them the sol-gel process is the most popular technique for preparing porous TiO_2 powder and thin film from alkoxide solutions containing organic polymer as template [11–14]. The effects of poly(ethylene glycol) (PEG) addition to the alkoxide solution on the photocatalytic activity and microstructure of the resultant coating have been studied [15, 16], indicating that PEG can perform as an effective pore-forming agent.

In the present paper, the synthesis of mesoporous TiO_2 has been carried out under hydrothermal conditions from the system of titanium sulfate [$Ti(SO_4)_2$] with urea [$CO(NH_2)_2$] as precipitating agent, and PEG as template. The influence of the amount and molecular weight of PEG on the surface morphology and

---

*Author to whom all correspondence should be addressed.

porosity was investigated as well as the effects of hydrothermal temperature and time. The obtained powder showed good performance for the degradation of gaseous formaldehyde. Hydrothermal synthesis with PEG is a convenient and efficient way to prepare mesoporous TiO_2 from $Ti(SO_4)_2$ water solution system.

2. Experimental

All the chemicals used were reagent-grade. The samples were prepared by the following method using titanium sulfate [$Ti(SO_4)_2$], urea [$CO(NH_2)_2$] and poly(ethylene glycol) (PEG). The synthesis was carried out using a 50 ml autoclave, provided the teflon liner, at 120, 140, 160°C respectively. About 35 ml $Ti(SO_4)_2$ solution was prepared and the concentration was 0.5 $mol{\cdot}l^{-1}$. The concentration of $CO(NH_2)_2$ was 1.0 $mol{\cdot}l^{-1}$. PEG with average molecular weights of 200 was used in the reaction. After the solutions were treated under hydrothermal conditions for 2, 4, 6, 8 h respectively, the precipitates were centrifugally separated and cleaned with deionized water thoroughly. The samples were obtained after the precipitates were dried at 80°C.

TGA and DTA analyses were performed on Dupont 1090 thermal analyzer. The atmosphere was air and the heating rate was 10°C/min. IR spectra were obtained in Perkin-Elmer 2000 FT-IR instrument. X-ray Diffraction (XRD) experiments were carried out in Bruker D8 Advance X-ray Powder Diffractometer with Cu K_α radiation. The Raman spectra were recorded on a Renishaw Ramanscope using an Argon-ion laser (514 nm) as the light source. The surface morphology was measured using Hitachi H-800 Transmission Electron Microscopy (TEM). The accelerating voltage of electron beam was 200 kV. The surface area and the pore distribution were determined by N_2 adsorption isotherms using an ASAP 2010 Micromeritics. The mesoporous TiO_2 powder was dip-coated on the glass particles and the evaluation of photocatalytic activity was carried out in a quartz tubular reactor by measuring the photo-induced degradation of gaseous formaldehyde using Gas Chromatograph (GC) to determine the photo-degraded products. The power and the wavelength of the UV light were 8 W and 253.7 nm, respectively.

3. Results and discussion

3.1. The formation and the thermal decomposition analysis

The hydrothermal procedure of $Ti(SO_4)_2$ and $CO(NH_2)_2$ to form TiO_2 could be formulated as follows:

$$Ti(SO_4)_2 + 2CO(NH_2)_2 + 6H_2O \\ \rightarrow Ti(OH)_4 \downarrow + 2(NH_4)_2SO_4 + 2CO_2 \uparrow$$

The molecule of PEG acted as a template with lots of hydroxyl (—OH) in its molecular chain. By adding PEG into the hydrothermal system, the effect of hydrogen bond was strengthened and $(HO)_3$-$(Ti$-$O)_n$-H sol could form around the micelle. In the hydrolysis process, the PEG segments could form crown-ether-type complexes with Ti^{4+} by weak coordination bonds. Thus the ordered inorganic/polymer composites were obtained through the self-assembling of the complexes [17]. Since PEG is a kind of water-soluble polymer, it could be almost eliminated by centrifugal separating the precipitation for more than 5 times. The preparation result was investigated using IR analysis as shown in Fig. 1. The IR spectra of the samples added with different amount of PEG were compared with that of pure PEG 200. In the spectrum of PEG 200, the absorption peaks at 3418 and 1651 cm^{-1} were attributed to —OH bond. The strong absorption peak at 2874 cm^{-1} and the peaks at 1455 and 1350 cm^{-1} were attributed to $—CH_2$ in molecular chain. The peaks at 1100 cm^{-1} were attributed to C—O bonds. The IR spectra of the samples added with 1% PEG 200 and the sample with PEG free are quite similar. The peaks at 3418 and 1651 cm^{-1} represent the —OH group adsorbed to the surface of TiO_2. The typical peaks of PEG 200 are too weak to be examined, which indicates that PEG 200 has been eliminated completely by centrifugal separation and washing. However, the double peaks at 1100 cm^{-1} appear obviously when the amount of PEG 200 increased to 25%, which represents the overlap of the stretching modes of Ti—O bonds in the inorganic polymer and C—O bonds in the remained PEG. This also suggests that it is difficult to remove the PEG 200 completely when the initial concentration is high. Compared with the calcination method, the centrifugal separation and washing can effectively remove the additive PEG 200 of low concentration from the products without destroying the mesoporous structure.

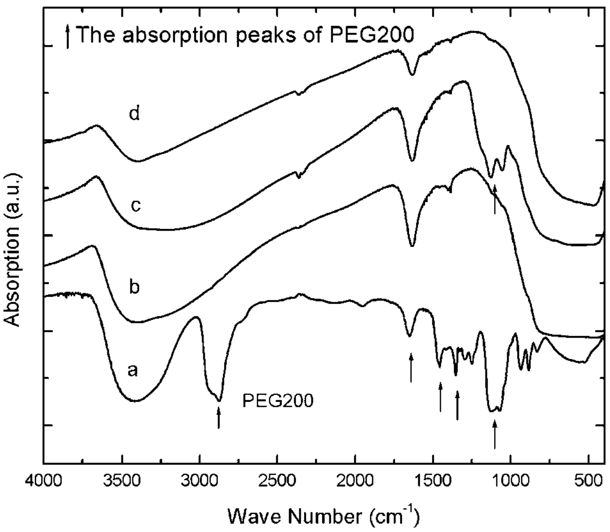

Figure 1 The IR spectra of the different samples compared with that of PEG 200: (a) pure PEG 200 sample, (b) PEG 200, 1%, (c) PEG 200, 25%, and (d) PEG free.

The results of the TGA-DTA analysis of the sample confirmed the conclusion (Fig. 2). There was a slide in the DTA curves, which implied that there was no obvious exothermal or isothermal phenomenon when the sample was heated till 900°C. There was only one weight-loss region from room temperature to 120°C. This resulted from the removing of absorbed H_2O and —OH group. The gradual weight loss up to 500°C

TABLE I The dependence of the crystal sizes derived from XRD patterns and the Raman shift of the main peak on the PEG amount, time and temperature

Concentration of PEG 200 (V%)	4% 120°C, 2 h	15% 120°C, 2 h	20% 120°C, 2 h	20% 120°C, 8 h	20% 160°C, 2 h
Average crystal size, Dc (nm)	10.58	6.11	5.92	13.06	12.51
Raman shift of the main peak (cm^{-1})	148	–	151	147	147

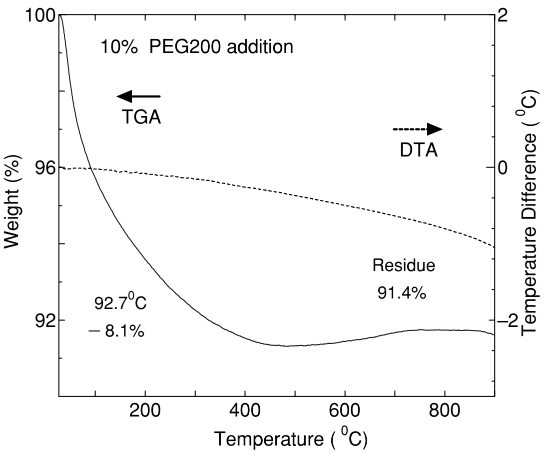

Figure 2 Typical TGA-DTA results of the sample added with 10% amount of PEG 200.

showed the decomposition of the residual PEG. The TGA-DTA analysis of other samples was the same. It was concluded that the synthesized powder consisted of almost pure TiO_2 without any organic component.

3.2. The effect of PEG concentration on the crystallization

The influence of the amount of the template PEG 200 on the crystallization of mesoporous TiO_2 powder has been investigated using XRD as shown in Fig. 3. All the marked peaks are attributed to the characteristic diffraction peaks of anatase phase. As the amount of PEG 200 increased, the characteristic peaks weakened and broadened, indicating that the crystalline of TiO_2 powder became less perfect. This may be due to the increase of the inorganic polymerization degree. The average crystal sizes can be determined from the XRD pattern parameters according to the Scherrer equation: $Dc = K\lambda/\beta\cos\theta$. Dc is the average crystal size, K is the Scherrer constant equal to 0.89, λ is the X-ray wavelength equal to 0.1542 nm, β is the full width at half-maximum (FWHM) and θ is the diffraction angle. According to the results in Table I, the average crystal sizes decrease with the increase of the added PEG 200.

The influences of the hydrothermal temperature and time on the crystallization of TiO_2 powder were also studied by XRD (Fig. 4). As the temperature increased to 160°C, the characteristic peaks of the anatase structure intensified and sharpened significantly and some main peaks split into halves. The average crystal sizes were increased up to 12 nm. It can be concluded that the crystalline phase of anatase TiO_2 became more perfect with the hydrothermal temperature. The effect of the reaction time was the same as that of the temperature.

The crystallization of the samples added with different amount of PEG 200 was also investigated using Raman spectroscopy (Fig. 5). The Raman spectra of different samples all exhibited only bands that were attributable to anatase phase: 146, 397, 519 and 641 cm^{-1} [18, 19]. It has been reported that the small changes in Raman line position and broadening are due to differences in the crystal distribution and pore size [20]. When the crystal size decreasing, the peak broadens asymmetrically (high frequency), shifts to the blue and decreases in intensity due to the quantum size effect. The results in Table I and Fig. 5 also reveal that lower temperature, shorter time and more PEG additive are important factors to obtain TiO_2 with smaller crystal sizes. These results are consistent with the XRD patterns above.

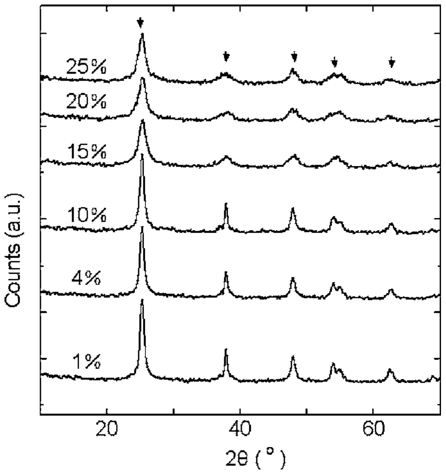

Figure 3 The XRD spectra of the samples added with different amount of PEG 200.

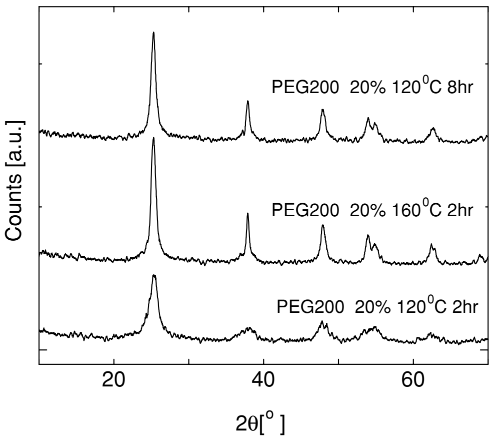

Figure 4 The XRD spectra of the samples obtained under different conditions.

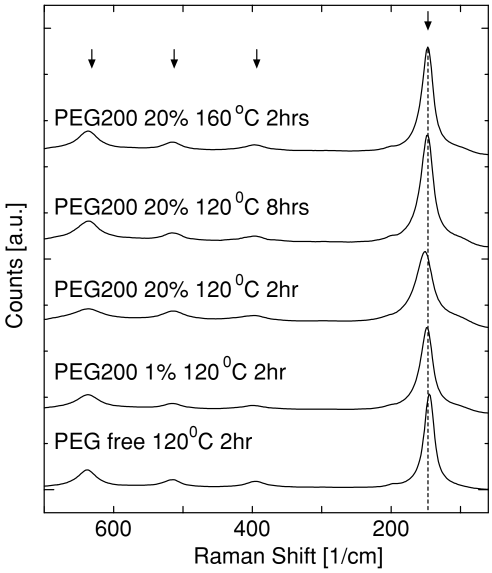

Figure 5 The Raman spectra of different samples.

3.3. The surface morphology of the mesoporous samples

The surface morphology of the mesoporous TiO_2 powders was studied using TEM. Without addition of PEG into the hydrothermal solution, the obtained powder has no mesoporous structure (Fig. 6a). The grain size of the powder was about 10–20 nm. After 1% PEG 200 was added, some cylindrical to hexagonal-shaped channels were observed. But there were still many separate grains. As the amount of PEG 200 increased, the mesoporous structure spread. The pore size increased and the channels with relative regular diameters were connected together when the amount increased to 10% (Fig. 6b). Such structure with channels is helpful for chemical reactions.

The influences of the hydrothermal temperature and time on the surface morphology were also investigated. When the time of the hydrothermal preparation increased up to 6 h, the mesoporous structure was destroyed and the TiO_2 grain appeared. The same phenomenon was observed when the temperature increased to 160°C.

The above results explained that PEG provided a useful and convenient pathway to synthesis mesoporous TiO_2 powder and it is important to choose an optimum amount of PEG at an appropriate temperature.

3.4. The porous structure of the TiO_2 powder

All isotherm plots of the TiO_2 samples using different amount of PEG 200 as templates belonged to the same isothermal type of the physical adsorption of gases by mesoporous solids [21]. Fig. 7 presents the N_2 adsorption isotherms and the corresponding BJH pore size distribution curves for the samples added with 10% and 20% PEG 200. The pore size distribution is calculated using the Kelvin Equation.

The pore size distribution of the sample added with 10% PEG 200 was fairly wide. The mesopores were not uniform and reached at about 18 nm. When 20% PEG 200 was added, the pore size became narrow and decreased. This result agreed with that of TEM. But there still existed some micropores in such system.

The surface area, the pore distribution and the cumulative pore volume of some samples were determined by N_2 adsorption isotherms listed in Table II. The differences in the BET surface areas were relatively small,

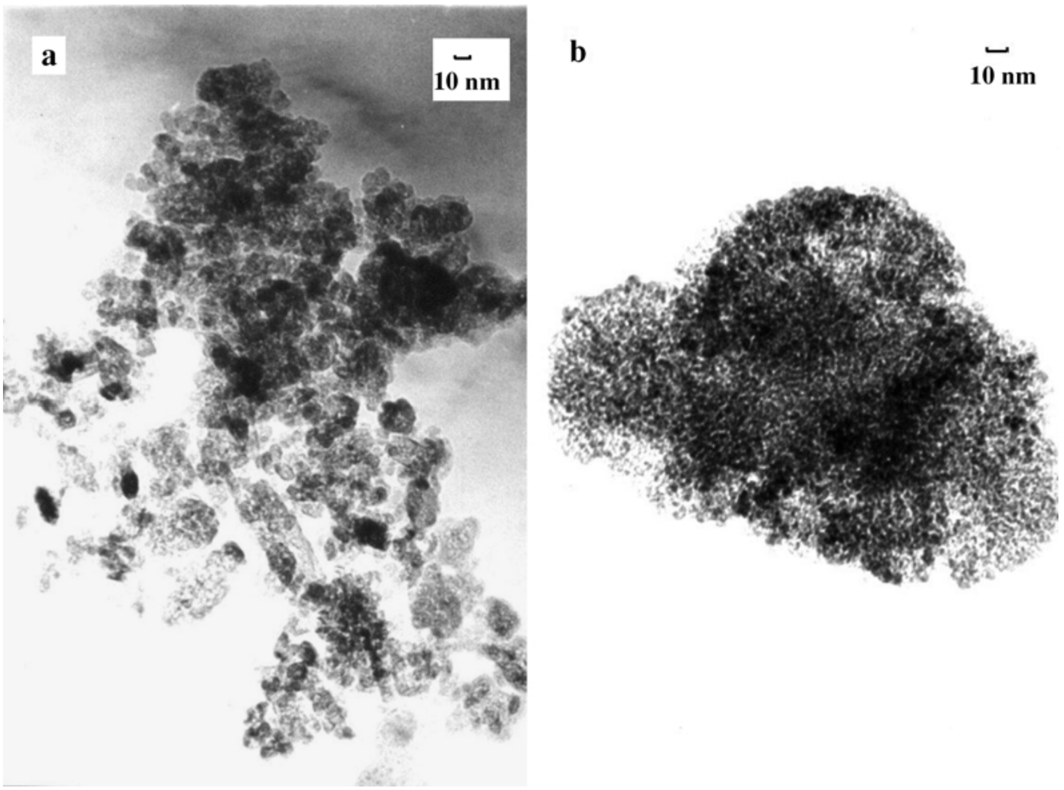

Figure 6 The cross-sectional bright field TEM images of the different samples (a) PEG free and (b) PEG 200, 10%, 120°C, 2 h.

TABLE II The surface area, average pore diameter and cumulative pore volume of the sample added with different amount of PEG 200

Concentration of PEG 200 (V%)	4	10	15	20
BET surface area ($m^2 \cdot g^{-1}$)	198.09	233.22	234.09	172.43
BJH desorption average pore diameter (4V/A) (nm)	9.46	9.94	6.31	6.63
BJH desorption cumulative pore volume of pores ($cm^3 \cdot g^{-1}$)	0.42	0.40	0.16	0.09

which was attributed to the existence of micropores in the samples. The surface area of the sample added with 10% PEG 200 (233.22 m^2/g) was relatively high compared with other samples. It was also observed that the average pore diameter of this sample reached a maximum of 9.94 nm. This result suggested that the amount of 10% of PEG 200 was the optimum choice to produce the mesoporous TiO_2 powder.

3.5. The photocatalytic activity of the mesoporous TiO_2 powder

The TiO_2 sample with 10% PEG 200 as template was adopted to evaluate the photocatalytic activity for the degradation of gaseous formaldehyde. Totally only about 3 mg TiO_2 was dip-coated on the 20 ml glass balls (diameter 3–4 mm). The original concentration of gaseous formaldehyde was about 1800 ppm and the flow rate was about 160 ml/min. Fig. 8 shows the

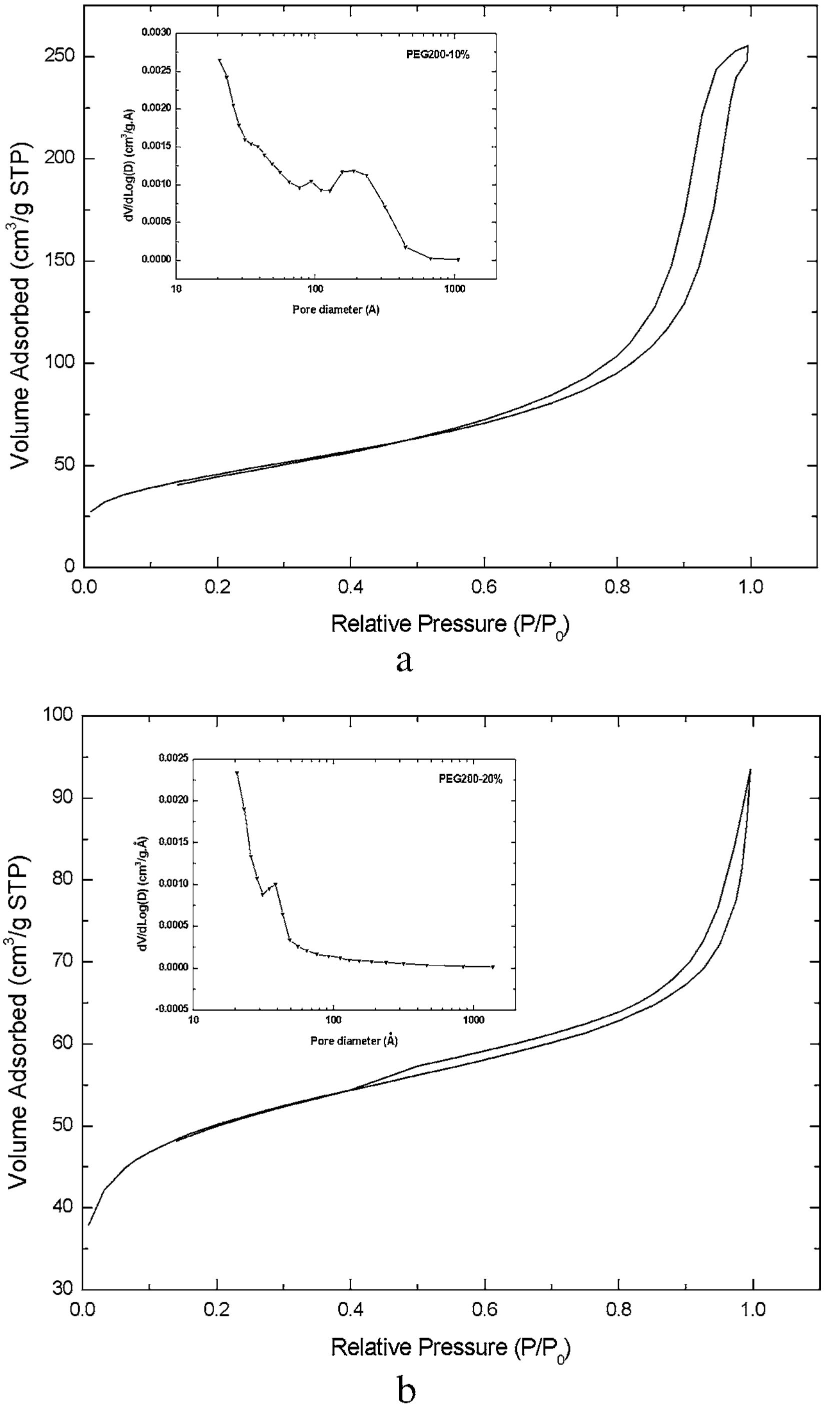

Figure 7 N_2 adsorption and desorption isotherms and the pore size distributions of the samples added with different amount of PEG 200: (a) PEG 200, 10% and (b) PEG 200, 20%.

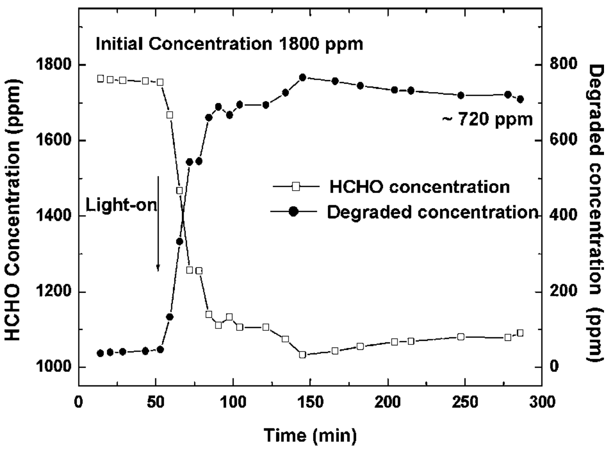

Figure 8 The activity plot of the sample added with 10% PEG 200.

formaldehyde concentration as a function of the irradiation time. The intermediate product of methanoic acid was detected during the photodegradation. About 1100 ppm gaseous formaldehyde was degraded as CO_2 and H_2O when the reaction reached the equilibrium point at 80 min. The degradation rate reached at about 61%. It has been established that highly mobile electron-hole pairs can be created when the TiO_2 semiconductor is irradiated with UV light of wavelength shorter than 380 nm. These carriers can be trapped by surface adsorbed molecules after migrating to the surface, leading to oxidation and reduction processes. It supposed that the three-dimensional mesoporous structure increased the surface area and would benefit molecular diffusion for applications such as catalysis, which resulted in the high photocatalytic activity.

4. Conclusion

Anatase TiO_2 with mesopore structure was synthesized using PEG as template under hydrothermal conditions from inorganic salts. The increase of the amount of PEG template would lead to the formation of non-perfect anatase structure and the decrease of the pore sizes. The increase of hydrothermal temperature or time did harm to the formation of mesoporous structure. The mesoporous TiO_2 sample showed good photocatalytic performance during the photodegradation of gaseous formaldehyde.

Acknowledgements

This work was partly supported by Chinese National Science Foundation (20071021), Trans-Century Training Program Foundation for the Talents by the Ministry of Education (MOE), P.R. China and supported by the Excellent Young Teacher Program of MOE, P.R. China.

References

1. K. ISHIZAKI, S. KOMARNENI and M. NANKO, "Porous Materials: Process Technology and Applications" (Kluwer Academic Publishers, 1998).
2. I. SOPYAN, M. WATANABE, S. MURASUWA, K. HASHIMOTO and A. FUJISHIMA, *J. Photochem. Photobiol. A Chem.* **98** (1996) 79.
3. L. SAADOUN, J. A. AYLLON, J. JIMERNEZ-BECERRIL, J. PERAL, X. DOMENECH and R. RODRIGUEZ-CLEMENTE, *Appl. Catal.* B **21** (1999) 269.
4. K. BYRAPPA, K. M. LOKANATHA RAI and M. YOSHIMURA, *Environ. Technol.* **21** (2000) 1085.
5. KRISHNANKUTTY-NAIR P. KUMAR, *Appl. Catal.* A **119** (1994) 163.
6. J. ZHAO, Z. WANG, L. WANG, H. YANG and M. ZHAO, *Mater. Chem. Phys.* **63** (2000) 9.
7. DAVID M. ANTONELLI and JACKIE Y. YING, *Angew. Chem. Int. Ed. Engl.* **34**(18) (1995) 2014.
8. A. ZABAN, S. T. ARUNA, S. TIROSH, B. A. GREGG and Y. MASTAI, *J. Phys. Chem.* B **104** (2000) 4130.
9. K. SRIKANTH, MD. M. RAHMAN, H. TANAKA, K. M. KRISHNA, T. SOGA, M. K. MISHRA, T. JIMBO and M. UMENO, *Solar Energy Mater. Solar Cells* **65** (2001) 171.
10. Y. ZHU, L. ZHANG, C. GAO and L. CAO, *J. Mater. Sci.* **35** (2000) 4049.
11. T. SUN and J. Y. YING, *Angew. Chem. Int. Ed.* **37**(5) (1998) 664.
12. E. STATHATOS, D. TSIOURVAS and P. LIANOS, *Colloids Surf.* A **149** (1999) 49.
13. S. A. BAGSHAW, E. PROUZET and T. J. PINNAVAIA, *Science* **269** (1995) 1242.
14. P. YANG, D. ZHAO, D. I. MARGOLESE, B. F. CHMELKA and G. D. STUCKY, *Nature* **396** (1998) 152.
15. J. YU, X. ZHAO, J. DU and W. CHEN, *J. Sol-Gel Sci. Technol.* **17** (2000) 163.
16. K. KAJIHARA, K. NAKANISHI, K. TANAKA, K. HIRAO and N. SOGA, *J. Amer. Ceram. Soc.* **81**(10) (1998) 2670.
17. F. E. J. BAILEY and J. V. KOLESKE, "Alkylene Oxides and Their Polymers" (Marcel Dekker, New York, 1990).
18. U. BALACHANDRAN and N. G. EROR, *J. Solid State Chem.* **42** (1982) 276.
19. I. SOPYAN, M. WATANABE, S. MURASAWA, K. HASHIMOTO and A. FUJISHIMA, *J. Photochem. Photobiol. A Chem.* **98** (1996) 79.
20. S. KELLY, F. H. POLLAK and M. TOMKIEWICZ, *J. Phys. Chem.* B **101** (1997) 2730.
21. S. J. GREGG and K. S. W. SING, "Surface Area and Porosity." 2nd ed. (Academic Press Inc. Ltd., London, 1982).

Received 4 December 2002
and accepted 7 July 2003